

December 01, 2002

Variation in material parameters for hexagonal barium ferrite films on (111) magnesium oxide as a function of oxygen pressure

S. D. Yoon

C. Vittoria
Northeastern University

S. A. Oliver

Recommended Citation

Yoon, S. D.; Vittoria, C.; and Oliver, S. A., "Variation in material parameters for hexagonal barium ferrite films on (111) magnesium oxide as a function of oxygen pressure" (2002). *Electrical and Computer Engineering Faculty Publications*. Paper 135.
<http://hdl.handle.net/2047/d20002306>



Variation in material parameters for hexagonal barium ferrite films on (111) magnesium oxide as a function of oxygen pressure

S. D. Yoon, C. Vittoria, and S. A. Oliver

Citation: *J. Appl. Phys.* **92**, 6733 (2002); doi: 10.1063/1.1521525

View online: <http://dx.doi.org/10.1063/1.1521525>

View Table of Contents: <http://jap.aip.org/resource/1/JAPIAU/v92/i11>

Published by the [American Institute of Physics](#).

Related Articles

Large anisotropic remnant magnetization tunability in (011)-La_{2/3}Sr_{1/3}MnO₃/0.7Pb(Mg_{2/3}Nb_{1/3})O₃-0.3PbTiO₃ multiferroic epitaxial heterostructures

Appl. Phys. Lett. **100**, 043506 (2012)

Induced magnetic anisotropy and spin polarization in pulsed laser-deposited Co₂MnSb thin films

J. Appl. Phys. **111**, 023903 (2012)

Room temperature ferromagnetism in transparent Fe-doped In₂O₃ films

Appl. Phys. Lett. **100**, 032404 (2012)

Chemical ordering of FePt films using millisecond flash-lamp annealing

J. Appl. Phys. **111**, 023902 (2012)

Probing origin of room temperature ferromagnetism in Ni ion implanted ZnO films with x-ray absorption spectroscopy

J. Appl. Phys. **111**, 013715 (2012)

Additional information on *J. Appl. Phys.*

Journal Homepage: <http://jap.aip.org/>

Journal Information: http://jap.aip.org/about/about_the_journal

Top downloads: http://jap.aip.org/features/most_downloaded

Information for Authors: <http://jap.aip.org/authors>

ADVERTISEMENT

LakeShore Model 8404 developed with **TOYO Corporation**
NEW AC/DC Hall Effect System Measure mobilities down to 0.001 cm²/V s

Variation in material parameters for hexagonal barium ferrite films on (111) magnesium oxide as a function of oxygen pressure

S. D. Yoon^{a)} and C. Vittoria

Department of Electrical and Computer Engineering, Northeastern University, Boston, Massachusetts 02115

S. A. Oliver

Center for Subsurface Sensing and Imaging Systems, Northeastern University, Boston, Massachusetts 02115

(Received 31 May 2002; accepted 22 September 2002)

This work examines the material characteristics and magnetic properties of hexagonal M-type barium ferrite ($\text{BaFe}_{12}\text{O}_{19}$) films deposited by pulsed laser ablation deposition onto (111) magnesium oxide substrates at different oxygen growth pressures. X-ray diffraction data showed the lattice constant of the film grown at 300 mTorr $c=23.23 \text{ \AA}$ increased to $c=23.30 \text{ \AA}$ for the film grown at 20 mTorr. The saturation magnetization ranged from 4.03 to 4.33 kG and the magnetic uniaxial anisotropy field ranged from 16.73 to 19.49 kOe as the oxygen pressure was varied from 10 to 300 mTorr. The narrowest ferrimagnetic resonance (FMR) linewidths (ΔH) for as-produced films were obtained for the 10 mTorr films, where $\Delta H=0.39 \text{ kOe}$. Films grown with oxygen pressure at 200 mTorr or higher showed two distinct resonance modes, which exhibited $\Delta H_1 \geq 0.90 \text{ kOe}$ and $\Delta H_2 \geq 1.10 \text{ kOe}$ at 59 GHz for a film deposited at 925 °C. The FMR linewidths for this film decreased to $\Delta H_1=0.52 \text{ kOe}$ and $\Delta H_2=0.45 \text{ kOe}$ after annealing the film at 1000 °C for 1 h. These results indicate that thick films grown at higher oxygen pressures have magnetic parameters closer to bulk values, but also show larger magnetic losses than films grown at lower oxygen pressures. © 2002 American Institute of Physics. [DOI: 10.1063/1.1521525]

I. INTRODUCTION

The growth of hexagonal structure M-type ferrite ($\text{BaFe}_{12}\text{O}_{19}$, BaM) films for usage in planar microwave devices has been studied by a number of research groups. Because of the large uniaxial magnetocrystalline anisotropy field (H_A) present in BaM ($H_A \sim 17 \text{ kOe}$ for bulk material),^{1,2} this material has been identified as an excellent candidate for deployment in nonreciprocal millimeter wave devices, such as circulators, phase shifters, and isolators.³ However, the incorporation of BaM films in these applications is still limited by the following reasons: (1) It is difficult to grow high quality epitaxy BaM films greater than 50 μm thick; (2) high cost of production due to the fact that substrates of the hexagonal crystal symmetry are not readily available and are very expensive; (3) the technology for integrating BaM films with other dielectric and/or superconductor materials is still at a rudimentary stage.

To date, near intrinsic quality low ferrimagnetic resonance (FMR) linewidth (ΔH) has been measured⁴ on thick BaM films, $\sim 45 \mu\text{m}$ thick, produced by the liquid phase epitaxy (LPE) deposition technique. Since the LPE technique has produced thick BaM films with ΔH of 0.03 kOe, we tried to duplicate these results with the pulsed laser ablation deposition (PLD) technique. PLD has become a well-established technique to grow oxide films, and has been used for depositing high temperature superconducting, ferroelectric, and ferrimagnetic films. PLD technique was recently used to deposit thick, and highly c -axis oriented BaM films ($\sim 40 \mu\text{m}$) onto (111) magnesium oxide (MgO) substrates.⁵

Postannealing of as-produced thick BaM film and removal of part of the MgO substrates helped to reduce the FMR ΔH of these films.⁶ Previous research examined effects of growth oxygen pressure (PO_2) on the properties of BaM films on (0001) sapphire (Al_2O_3) substrates.⁷ In this work we extend this previous work⁷ by examining the effects of PO_2 on BaM films on (111) MgO substrates.

Previous work on hexaferrite films deposited onto (0001) Al_2O_3 showed films grown at $\text{PO}_2=300 \text{ mTorr}$ ($< 1 \mu\text{m}$) the lowest ΔH .⁸ In general, as produced BaM films ($1 \mu\text{m} \leq \text{films thickness} \leq 30 \mu\text{m}$) on (111) MgO substrates showed higher ΔH , $\sim 0.4\text{--}0.7 \text{ kOe}$, than the BaM films on sapphire substrates.⁶ ΔH of 0.06 kOe was measured on a BaM films on (111) MgO, where the film ($\sim 3 \mu\text{m}$) was annealed at 1000 °C for 2 h in air.⁶ The mechanisms for microwave loss in hexaferrites have been investigated by others, who considered the effects of eddy current losses,⁸ surface inhomogeneities,^{8,9} and material inhomogeneities such as oxygen deficiencies, voids, stacking faults, and defects. However, the correlation between the growth parameters of BaM films and the resulting structural and magnetic properties are still relatively unknown. Moreover, despite the successes in growing highly c -axis oriented thick BaM films on (111) MgO at lower PO_2 ($\text{PO}_2=20 \text{ mTorr}$), results obtained for growing thick BaM films ($> 10 \mu\text{m}$) at higher PO_2 have not yet been reported. Here we detail the growth pressure dependencies on the structural, magnetic, and microwave magnetic properties of thick BaM films on (111) MgO.

II. EXPERIMENT

An excimer laser was used for deposition, which was operating at 248 nm with a pulse energy of $\sim 400 \text{ mJ}$ and a

^{a)}Electronic mail: syoon@ece.neu.edu

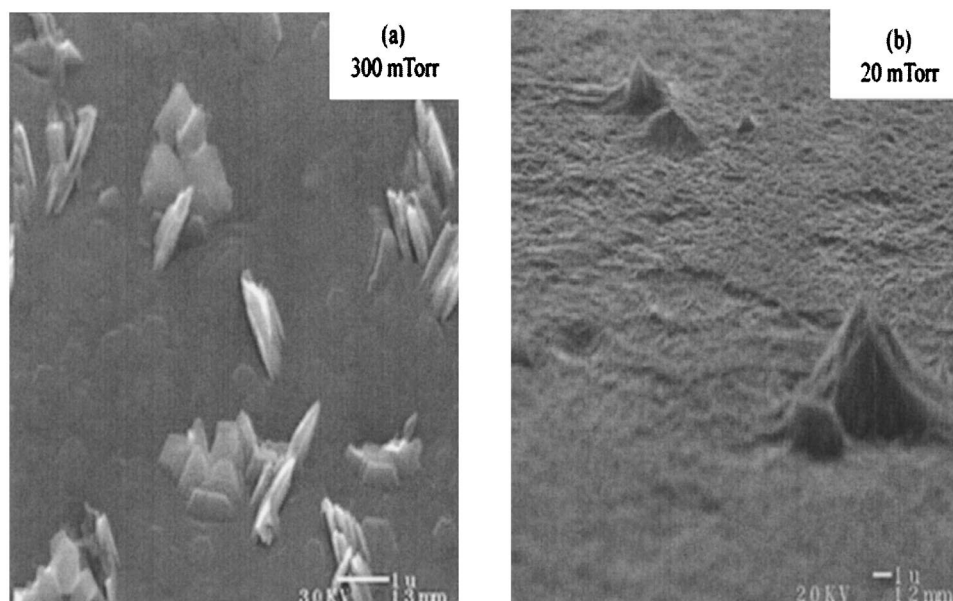


FIG. 1. SEM surface morphologies of the films deposited at (a) 300 mTorr and (b) 20 mTorr.

25 ns full width at half maximum pulse width. A commercially prepared BaM bulk target, having a density of 4.3 g/cm^3 , was used for ablating. Films were deposited onto polished $10 \times 10 \times 0.5 \text{ mm}$ (111) MgO substrates, which were cleaned by diluted nitric and acetic acid.^{6,9} The substrates were mounted by silver paint on a cylindrical block resistive heater, and the heater was placed 5 cm away from the rotating BaM target, and the laser beam was rastered across the target surface.

The substrate heater was placed in vacuum chamber, and then pumped down to a base pressure near 10^{-6} Torr before setting the substrate temperature to $925 \text{ }^\circ\text{C}$ and supplying the high purity oxygen (99.998%) gas. The oxygen pressure of the deposition in the chamber was varied from a lowest 10 mTorr to the maximum 300 mTorr before film deposition. The ablation target was cleaned by the excimer laser at a frequency of 10 Hz for 10 min before starting the film deposition. Each film was initially started at a slow deposition rate of 1 Hz for 10 min, before increasing the deposition rate to 5, 10, 20, and 30 Hz, so as to promote good film adhesion. The total deposition time was fixed at 40 min for each film. Selected films were annealed in air flow at $1000 \text{ }^\circ\text{C}$ for 1 h.

The surface morphologies and thicknesses of the film were measured by a scanning electron microscope (SEM). $2-\theta$ scan x-ray diffraction (XRD) spectra were measured for all the films. In addition, XRD rocking curves of the BaM (0008) plane were measured in order to examine the film mosaicity. Vibrating sample magnetometer (VSM) and torque magnetometer measurements were performed in order to analyze magnetic orientations and properties of the films. Ferrimagnetic resonance (FMR) measurements were performed using a shorted waveguide technique where a swept dc magnetic field was applied normal to the film plane, in the so-called perpendicular FMR configuration. FMR measurements were obtained from 40 to 60 GHz.

III. RESULTS AND DISCUSSION

Figure 1 shows SEM images for the BaM films grown at oxygen background pressures (PO_2) of 300 mTorr [Fig. 1(a)] and 20 mTorr [Fig. 1(b)]. Here the SEM image in Fig. 1(a) is typical of those pictured for all the BaM films grown at $\text{PO}_2 \geq 200$ mTorr, where the surface image consists of small sloped outgrowth and hexagonal growth patterns on the film surface (on-plane hexagonal pattern). c -axis misalignment relative to the film plane is evident from Fig. 1(a) as shown from the tilting of the hexagonal platelet. This type of growth is usually referred to as outgrowth. Normal growth is seen as the growth of regular hexagonal platelets on the film plane. Size of the outgrowth platelets ranged between 1 and $2 \text{ } \mu\text{m}$, where the on-plane hexagonal patterns or normal growth size range from ~ 0.5 to $1.0 \text{ } \mu\text{m}$. This result indicates in-plane growth rate for the outgrowth platelets were faster than the hexagonal platelets on the film plane. Therefore, eventually, the presence of such outgrowth platelets will affect the crystallographic properties of the film by disrupting epitaxy, cracks, voids, and defects. A typical SEM image for the BaM film grown at lower oxygen pressure ($\text{PO}_2 \leq 100$ mTorr) is shown in Fig. 1(b). In contrast to Fig. 1(a), fewer outgrowths are seen. In previous work, it was shown that highly oriented thick BaM films ($> 10 \text{ } \mu\text{m}$) on (111) MgO substrates can be grown by PLD at only lower oxygen pressure ($\text{PO}_2 \sim 20$ mTorr) with high substrate heater ($T_s > 900 \text{ }^\circ\text{C}$) temperature.⁵ Consequently, use of lower PO_2 during the film deposition by PLD technique is important factor for preparing highly c -axis oriented BaM films on (111) MgO substrates. The thickness of the films was measured from cross section SEM images and are listed in Table I. No surface cracks were observed in any of the BaM films for thickness ranging from 1 to $2 \text{ } \mu\text{m}$.

X-ray diffraction (XRD) measurements showed that the films were well oriented with c -axis normal to the film plane.

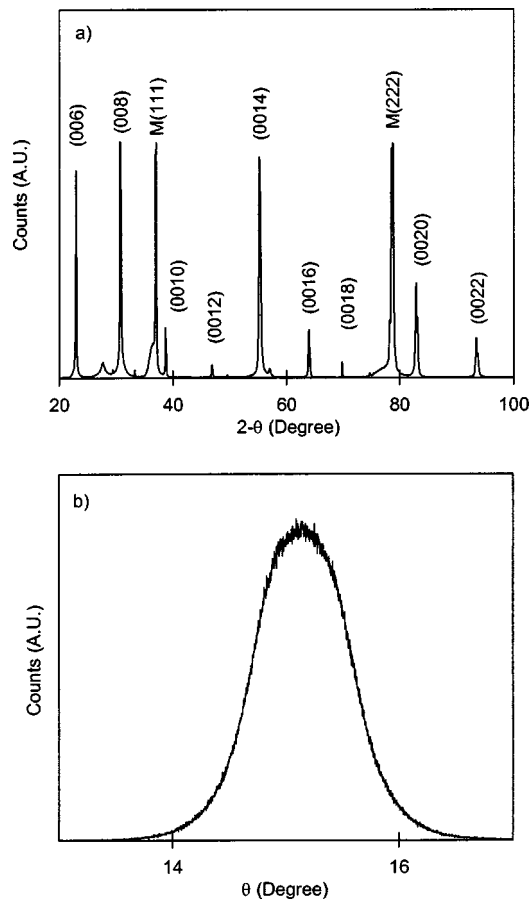


FIG. 2. (a) θ - 2θ XRD spectrum of BaM film deposited with 20 mTorr oxygen pressure. The peak “M” is the MgO substrate peak; (b) XRD θ scan rocking curve of BaM (0008) reflection.

A typical θ - 2θ scan XRD powder spectrum for the film grown at PO_2 of 20 mTorr is shown in Fig. 2(a). All significant reflections of the BaM (0001) planes are clearly apparent in the XRD spectrum for all films, which indicate that they had c -axis orientation. The peaks at both $2\theta = \sim 27^\circ$ and $\sim 57^\circ$ are identified as XRD from mounting clay material which is used for positioning the films on the XRD sample holder. A measure of the c -axis dispersion of the films was obtained by the full width at half-maximum (FWHM) of rocking curves taken on the (0008) diffraction peak. The rocking curve for the BaM film grown at 20 mTorr is shown in Fig. 2(b). The FWHM peak width of the film was found to be 0.864° . All of the FWHM results for the BaM

TABLE I. Various material and magnetic parameters for the BaM films grown at different oxygen pressures

PO_2 (mTorr)	Thickness (μm)	Lattice parameter (\AA)	XRD FWHM (deg)	Ave. ($4\pi M_s$) (kG)	Ave. (H_A) (kOe)
10	1.33 ± 0.10	23.304	0.692	4.03	16.73
20	1.72 ± 0.08	23.297	0.863	3.30	15.46
50	1.28 ± 0.08	23.278	1.034	3.59	16.08
100	1.02 ± 0.06	23.241	0.516	4.20	17.41
200	1.01 ± 0.08	23.222	0.786	4.29	18.95
300	1.04 ± 0.16	23.226	0.843	4.33	19.49

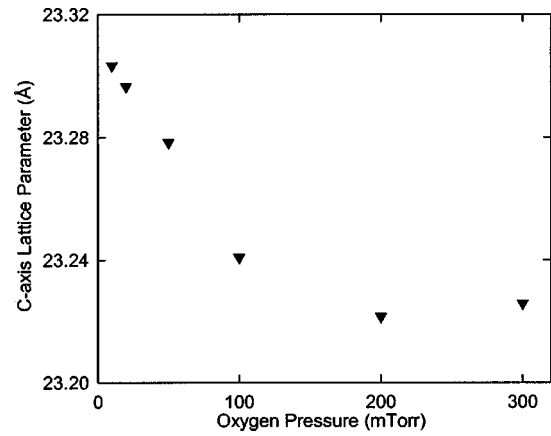


FIG. 3. c -axis lattice parameter measured from XRD data is shown as a function of oxygen pressure.

films are listed in Table I. The results show no trend for film mosaicity as a function of growth PO_2 . All FWHM values ranged between 0.510° and 0.890° except for the BaM film grown at 50 mTorr (FWHM = 1.03°).

Lattice constants (d_c) were deduced for the BaM films by fitting the centroid of the six most significant (0001) diffraction peaks to Bragg’s law. The results from the fits are shown in Fig. 3 as a function of growth PO_2 . The value of d_c given for bulk BaM ranges from 23.14 to 23.22 Å. In particular, the films grown at PO_2 near 200 mTorr or higher have d_c comparable to those of bulk BaM. However, the films grown at lower PO_2 ($PO_2 < 100$ mTorr) showed an increase in d_c value. This result was opposite to the results obtained for growing BaM films on (0001) Al_2O_3 substrates,⁷ where it was shown that the BaM films at lower PO_2 (10 and 20 mTorr have a d_c comparable to the BaM bulk values. These differences in d_c may be due to the presence of biaxial stress behavior between the BaM film and substrate as induced by the difference in thermal expansion coefficients between the BaM film and the substrate.^{6,7}

Magnetic hysteresis loops (M vs H) for the BaM films were measured by VSM with a maximum available applied magnetic field of 13 kOe. Figure 4 shows the hysteresis loops for the film grown at $PO_2 = 300$ mTorr [Fig. 4(a)] and at $PO_2 = 20$ mTorr [Fig. 4(b)]. Hysteresis loops were taken in both the out-of-plane (field applied normal to the film plane) and the in-plane (field applied along the film plane) geometry. In comparing the two hysteresis loops, it is seen that the hysteresis loop from Fig. 4(b) demonstrates better magnetic orientation than the hysteresis loop from Fig. 4(a). Indeed, VSM hysteresis for all films grown at $PO_2 \geq 200$ mTorr show similar hysteresis loop behavior to Fig. 4(a). Meanwhile, the films grown at lower PO_2 , have better magnetic orientation than the film grown at higher PO_2 , because the magnetic easy axis of the BaM coincided with the crystallographic c axis. The saturation magnetization ($4\pi M_s$) was deduced by two methods. The first method was to divide the EMU as measured by the VSM and multiply it by $4\pi/\Delta v$, where Δv was the volume of the sample. The other method is to determine the field at which technical saturation occurred or the field where the “knee” occurred in M (magnetization) versus

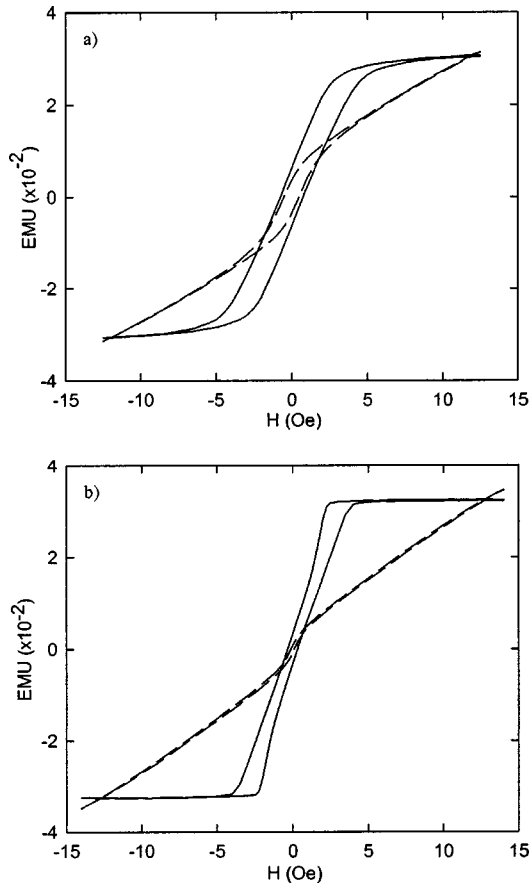


FIG. 4. Out-of-plane (solid line) and in-plane (dashed line) VSM hysteresis loops for the BaM films with (a) 300 mTorr, (b) 20 mTorr.

H (applied magnetic fields). In Table I we list the average $4\pi M_s$ based on these two methods of measurements. Here, from Table I, the values of $4\pi M_s$ decreased as the growing background PO_2 decreased. These lower $4\pi M_s$ values for the films grown at lower PO_2 was attributed to oxygen deficiencies in the films, since there is no trend between $4\pi M_s$ and the films' thickness (see Table I). Figure 4 also shows in-plane VSM hysteresis loop behaviors, where the M does not saturate to H of 13 kOe due to the large uniaxial anisotropy field (H_A) present in the BaM film. From the in-plane VSM hysteresis, M values at 13 kOe were $\sim 10\%$ larger than the values obtained from the VSM hysteresis measurements for the out-of-plane VSM measurement. This discrepancy was the result of placing the film closer to the measuring coils of the VSM magnets for the case of H field in the film plane, since the size of the film was significant ($1 \times 1 \text{ cm}^2$).

Values for loop squareness ($SQ = M_r/M_s$), where M_r is the remanent magnetization and M_s is the saturation magnetization, and coercive fields (H_c) were obtained from the hysteresis loops taken both along the film normal ($H_{c\perp}$) and along the film plane ($H_{c\parallel}$). No systematic variation was found in the value of ($H_{c\perp}$) vs PO_2 , but the value of $H_{c\parallel}$ does decrease systematically as a function of PO_2 . In general, the value of $H_{c\perp}$ may be related to crystallite size and domain size effects. However, it is hard to make any conclusion in this article due to insufficient data. The highest value

for $H_{c\perp}$ was obtained for the film grown at $PO_2 = 50 \text{ mTorr}$, but in general the films grown at higher PO_2 have larger $H_{c\perp}$ values. In addition, a distinct correlation between the value of $H_{c\parallel}$ and the FMR ΔH of the films was observed. Observation of a hysteresis in the $M-H$ curve when the field is applied along the hard axis (in-plane loop in this case) indicates that the crystal (or film) orientation is not ideally perfect but has some degree of spread of easy axis or evidence for local defects. These defects are increased with PO_2 pressure. This variation in local anisotropy produces non-uniformities in in-plane component of the magnetization. Thus, the increase in coercive field of the in-plane loop indicates that the crystalline quality of the film has become poorer or that the concentration of volume defects has increased, which in turn increases the FMR linewidth. Line-width broadening due to nonuniformities may be related to the two magnon relaxation processes from volume defects as developed originally by Clogston et al.¹⁰

Out-of-plane torque magnetometry measurements confirmed the excellent magnetic orientation present for these BaM films. All the films showed large torque upon rotating the H out-of-the-film plane, and showed near zero torque upon rotating H in-the-film plane. Figure 5(a) shows out-of plane torque for the film grown at $PO_2 = 300 \text{ mTorr}$, which is typical of all of the films. In this plot the 0° and 180° angles corresponding to the applied magnetic field being aligned relative to the film easy axis. In this plot the small different angular dependencies of the torque curves were observed for the rotation directions (clock or counterclockwise) at or near 90° and 270° , where the applied field in the film plane could not overcome the uniaxial anisotropy field. Figure 5(b) shows in-plane torque measurements for the films grown at $PO_2 = 300 \text{ mTorr}$ (solid line) and at $PO_2 = 20 \text{ mTorr}$ (symbol). A distinct sixfold symmetry is seen for the film grown at $PO_2 = 300 \text{ mTorr}$, while such a behavior was not observed in the films grown at $PO_2 \leq 100 \text{ mTorr}$.

Perpendicular FMR measurements were performed by applying a swept dc magnetic field normal to the film plane. Each film was placed into a waveguide such that the microwave magnetic field was maximum in-the-film plane and the static external magnetic field (H) was applied perpendicular to the film plane. The frequency was fixed for each H sweep, where FMR measurements were taken over the frequency range from 48 to 60 GHz. The perpendicular FMR condition is given by¹¹

$$\frac{\omega}{\gamma} = (H_r + H_A - 4\pi M_s),$$

where $\omega = 2\pi f$, $H_r \equiv$ the FMR field $H_A \equiv$ the uniaxial anisotropy field, and $\gamma = 2\pi(g \times 1.4 \times 10^6 \text{ Hz/Oe})$. An experimental value for the g factor was deduced from the slope of the FMR resonant frequency versus H_r , see Fig. 6. A g factor value of $g = 1.994 \pm 0.004$ was obtained from the slope [Fig. 6(a)]. The range of g values for the films grown at $PO_2 \leq 100 \text{ mTorr}$ was found to be from 1.966 to 1.994. This is in good agreement with $g \approx 2$ found for bulk samples.¹² Two values of g factor for films grown at $PO_2 \geq 200 \text{ mTorr}$ were obtained due to presence of multi-FMR modes from the

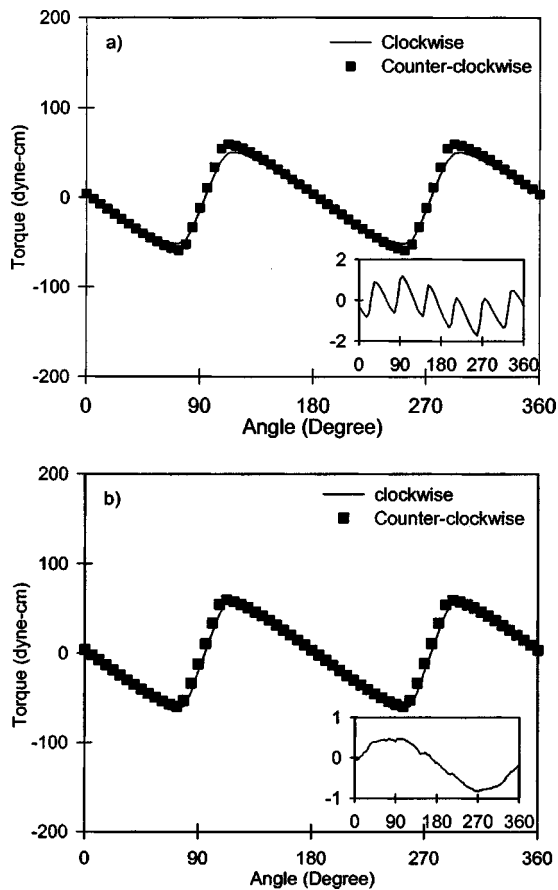


FIG. 5. Out-of-plane torque magnetometry measurements (solid line: clockwise, dashed line: counterclockwise measurement). Inserts show in-plane torque magnetometry measurements (clockwise measurement). (a) BaM film at 300 mTorr; (b) BaM film at 20 mTorr.

results of FMR resonant frequency versus H_r plots [see Fig. 7(a)]. Two distinct FMR modes were observed from the results. The range of the g factor for the first FMR mode was found to be from 1.756 to 1.859. However, the range of the g factor for the second FMR mode was from 1.961 to 1.970, much closer to the expected $g = 2$. Clearly, the $g \sim 1.8$ line is not an intrinsic line. This excitation may be localized at the interface between film and substrate, since the magnetization at the interface may be inhomogeneous. It is often the case for films which are highly inhomogeneous.^{13,14} The $g \sim 1.97$ line is intrinsic, since it agrees with the single lines observed in other films.¹² Figure 6(b) shows the relation between ΔH and PO_2 . ΔH decreased with decreasing PO_2 , where the lowest ΔH of 0.39 kOe was found for films grown at $PO_2 = 10$ mTorr [see insert in Fig. 6(a)]. This result indicates films grown at lower PO_2 have better microwave loss properties than films grown at higher PO_2 . Figure 7(b) shows FMR measurements for the as-produced film grown at $PO_2 = 200$ mTorr, and after annealing at 1000 °C for 1 h in air. The linewidths of both resonant modes were decreased by 45%–60% after the annealing, where the g factors for the film increased from 1.860 to 1.903 (for lowest field mode) and 1.961 to 1.988 (for the highest field mode). For very high quality films we would expect $g \sim 2$.^{4,12}

Values of $H_A = (2K)/M_S$ were measured on films by two different methods. In one technique we used the Miyajima

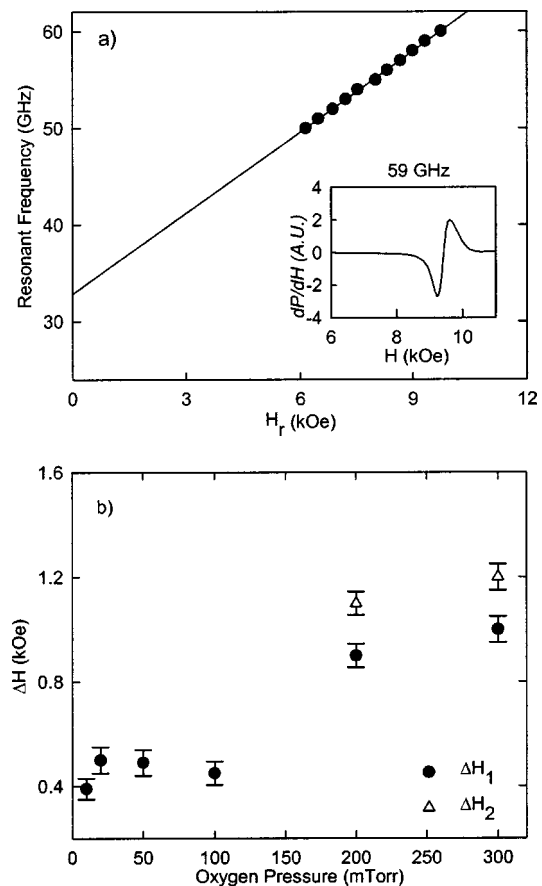


FIG. 6. (a) Resonant frequency vs applied magnetic field for the film grown at $PO_2 = 10$ mTorr. Insert shows linewidth for as-produced film at 59 GHz; (b) linewidth (ΔH) of as-produced BaM films, measured from the out-of-plane FMR spectrum, as a function of oxygen growth pressure.

method of torque analysis;¹⁴ in the other technique we fitted the resonance equation to measured frequency versus H_r , where the values of $4\pi M_s$ listed in Table I were used. Mean values of H_A yielded from these two methods are also listed in Table I. The values for the films grown at higher PO_2 (≥ 200 mTorr) have larger H_A values (~ 19.0 kOe) than that of bulk BaM ($H_A \sim 17.0$ kOe). The values for films grown at lower PO_2 (< 100 mTorr) have smaller H_A values (~ 15.0 kOe) than the bulk value of H_A . This result follows a similar trend to that found between $4\pi M_s$ and PO_2 . Clearly, H_A for the films was affected by oxygen deficiencies.

IV. CONCLUSIONS

In this article we are reporting on the growth conditions of hexaferrite ($BaFe_{12}O_{19}$, BaM) BaM films on (111) magnesium oxide (MgO) by the pulsed laser ablation (PLD) deposition technique. The morphology and magnetic properties of the films depended very strongly on the oxygen pressure during the deposition. Films deposited at high oxygen growth pressure (≥ 200 mTorr) showed better crystallographic ordering, where the lattice constant agreed with the bulk value. However, films deposited at higher oxygen growth pressure also showed significant outgrowths on the surface, while films deposited at lower oxygen growth pres-

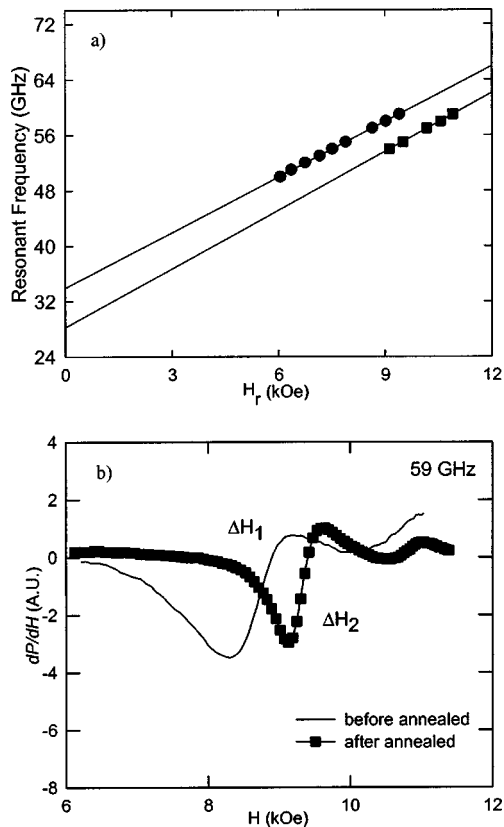


FIG. 7. FMR measurements for 200 mTorr film. (a) Resonant frequencies vs applied fields for film after annealing in air at 1000 °C for 1 h; (b) FMR spectrums for as-produced (solid line) and postannealed (symbol) film at 59 GHz.

sure showed fewer outgrowths. In order to make these films useful for device applications, they must be grown above certain thickness ($\sim 50 \mu\text{m}$ up to current device designs) while maintaining low magnetic losses. Given the presence of the outgrowths for such films, it may be difficult to grow epitaxial quality films on (111) MgO substrates thicker than

$10 \mu\text{m}$ by PLD technique using high oxygen pressure ($\text{PO}_2 \geq 200 \text{ mTorr}$). In addition, these films deposited at higher PO_2 showed larger magnetic losses and multiple ferrimagnetic resonance modes than those at lower PO_2 . One potential approach is to use lower PO_2 , which showed growth of thick BaM near $30 \mu\text{m}$ from previous work,⁷ even at similar deposition condition. In general postannealing reduced the magnetic losses and coercive field. In this work, the as-produced film ($\sim 1.3 \mu\text{m}$) grown at $\text{PO}_2 = 10 \text{ mTorr}$ showed the lowest magnetic losses where $\Delta H = 0.39 \text{ kOe}$ with their magnetic parameters similar to values of bulk BaM.

ACKNOWLEDGMENTS

This work was supported by the Office of Naval Research and the Defense Advanced Research Projects Agency under the 1996 Multidisciplinary University Research Initiative.

- ¹J. Smit and H. P. J. Wijn, *Ferrites* (Wiley, New York, 1959), p. 204.
- ²H. Kojima, in *Ferromagnetic Materials*, edited by E. P. Wohlfarth (North-Holland, New York, 1982), Vol. 3, p. 305.
- ³P. Shi, H. How, X. Zuo, S. D. Yoon, S. A. Oliver, and C. Vittoria, *IEEE Trans. Magn.* **37**, 2389 (2001).
- ⁴S. G. Wang, S. D. Yoon, and C. Vittoria, *J. Appl. Phys.* **92**, 6728 (2002).
- ⁵S. A. Oliver, S. D. Yoon, I. Kozulin, M. L. Chen, and C. Vittoria, *Appl. Phys. Lett.* **76**, 3612 (2000).
- ⁶S. D. Yoon, S. A. Oliver, P. Shi, X. Zuo, and C. Vittoria, *IEEE Trans. Magn.* **37**, 2389 (2001).
- ⁷S. A. Oliver, M. L. Chen, I. Kozulin, and C. Vittoria, *J. Magn. Magn. Mater.* **213**, 326 (2000).
- ⁸S. R. Shinde, S. E. Lofland, C. S. Ganpule, S. B. Ogale, S. M. Bhagat, T. Venkatesan, and R. Ramesh, *J. Appl. Phys.* **85**, 7459 (1999).
- ⁹S. D. Yoon, S. A. Oliver, and C. Vittoria, *J. Appl. Phys.* **91**, 7379 (2002).
- ¹⁰A.M. Clogston, H. Suhl, L.R. Walker, and P.W. Anderson, *Phys. Rev.* **101**, 903 (1956).
- ¹¹C. Vittoria, *Microwave Properties of Thin Magnetic Films* (World Scientific, Singapore, 1993), pp. 87–122.
- ¹²*Landolt-Börnstein, Numerical Data and Functional Relationships in Science and Technology*, edited by K.-H. Hellwege and A. M. Hellwege (Springer, Berlin, 1970), Vol. 4, Part B, p. 573.
- ¹³C. Vittoria and J. H. Schelleng, *Phys. Rev. B* **16**, 4020 (1977).
- ¹⁴H. Miyajima, K. Sato, and T. Mizoguchi, *J. Appl. Phys.* **47**, 4669 (1979).